A Three-Dimensional Biomechanical Evaluation of Quadriceps and Hamstrings Function Using Electrical Stimulation

Betsy V. Hunter, Darryl G. Thelen, and Yasin Y. Dhaher, *Senior Member, IEEE*

***Abstract*—Neurological disorders such as stroke impair locomotor control and result in abnormal 3-D gait kinematics. Establishment of effective rehabilitation strategies requires an understanding of how individual muscles contribute to pathological movement. Forward dynamic simulations account for complexities of interjoint coupling and can be used to predict dynamic muscle function. However to date, limited experimental validations of dynamic models have been performed. Our objective was to measure 3-D movement induced by the biceps femoris (BF), rectus femoris (RF), and vastus lateralis (VL) in limb configurations corresponding to the swing phase of gait, and to assess the biomechanical factors that affect dynamic function. Subjects were positioned in a robotic gait orthosis that included a compliant interface. Electrical stimulation was introduced into individual muscles while induced hip and knee joint movements were recorded. Measured hip to knee sagittal plane acceleration ratios were consistent with dynamic musculoskeletal model simulations. However RF and VL induced substantially larger frontal plane hip movements than model-based predictions. Sensitivity analyses on musculoskeletal model parameters revealed that muscle function depends primarily on moment arm assumptions. Though generic musculoskeletal models are suitable for predicting sagittal plane muscle function, improvements in moment arm accuracy are essential for investigation of 3-D pathological gait.**

***Index Terms*—Biarticular muscle, dynamic function, musculoskeletal modeling, three-dimensional muscle function.**

I. Introduction

GAIT rehabilitation strategies following a neurological disease, such as stroke, often include interventions that are intended to alter muscle force production, specifically during the swing phase of gait [1]. For example, pharmacological injections [2]–[5] can be used to weaken spastic muscles whereas functional electrical stimulation (FES) can be used to enhance active contraction forces [6]–[9]. These targeted interventions are generally guided by the perceived function of a muscle as derived from its anatomical organization. Though several interventions have achieved successful local muscular response, global functional improvements tend to be inconsistent and transient [10], [11]. For instance, following injection of botulinum toxin to treat rectus femoris (RF) spasticity in the stroke population, one group observed significant increase in gait velocity [3] while others did not [12], [13]. These conflicting functional outcomes may, in part, reflect an incomplete understanding of muscle function during walking.

Musculoskeletal modeling studies suggest that muscle function is highly dependent on dynamic coupling in the multi-degree-of-freedom (dof) musculoskeletal system [14]–[19]. For example, Arnold *et al.* found that two uniarticular muscles, iliopsoas and vasti, have the potential to generate large accelerations about joints they do not span [20]. In addition, dynamic models suggest that the biarticular RF may accelerate both the knee and hip into extension during the initiation of the swing phase of gait, with the action at the hip being directly opposite to the muscle's anatomically perceived role as a hip flexor [14], [21].

Recent empirical studies have verified the complex and often counterintuitive behavior of muscles in multi-joint systems. For example, members of our group used an FES-perturbation approach to show that the RF can induce hip extension in a side-lying posture [22], which is opposite to its anatomically perceived role as a hip flexor. Stewart *et al.* [23] used FES to augment plantarflexor muscle force during gait and clearly showed different function for the uniarticular soleus and the biarticular gastrocnemius about the ankle compared to static behaviors. FES was also used to investigate the changing role of the hamstrings muscles during quiet crouch standing [24]. Although these *in vivo* experiments indeed confirm several complexities of dynamic muscle function, the analyses were constrained to planar movements. However, the capability of muscles to contribute to motion in planes secondary to that of their primary function is also important to consider, particularly in pathological gait conditions.

Accordingly, we used an electrical stimulation protocol to obtain quantitative *in vivo* measurements of 3-D function of the biarticular RF and biceps femoris long head (BF) at postures representative of the swing phase of gait. We also evaluated the uniarticular vastus lateralis (VL) to better understand the role intersegmental coupling plays on the RF muscle function at the hip joint. Considering the inherent mechanical interactions

Manuscript received September 24, 2008; revised December 22, 2008; accepted January 07, 2009. First published February 03, 2009; current version published April 08, 2009. This work was supported in part by the Searle Fund, in part by the National Science Foundation Graduate Research Fellowship, in part by the American Heart Association Predoctoral Fellowship 0810115Z, and in part by the U.S. Department of Education, National Institute on Disability and Rehabilitation Research Field Initiated under Grant H133A990008.

B. V. Hunter is with the Biomedical Engineering Department, Northwestern University, Evanston, IL 60208 USA (e-mail: b-hunter@northwestern.edu).

D. G. Thelen is with the Mechanical Engineering Department, University of Wisconson-Madison, Madison, WI 53706 USA (e-mail: thelen@engr.wisc.edu).

Y. Y. Dhaher is with the Department of Biomedical Engineering and the Department of Physical Medicine and Rehabilitation, Northwestern University, Evanston, Il 60208 USA and also with the Sensory Motor Performance Program, Rehabilitation Institute of Chicago, Chicago, IL 60611 USA (e-mail: y-dhaher@northwestern.edu).

Digital Object Identifier 10.1109/TNSRE.2009.2014235

1534-4320/$25.00 © 2009 IEEE

Authorized licensed use limited to: Queens University. Downloaded on February 23,2010 at 15:43:07 EST from IEEE Xplore. Restrictions apply.

across segments, we hypothesized that the VL and RF would accelerate the hip into extension, contrary to their anatomical organizations. Furthermore, we hypothesized that RF and BF (biarticular muscles) would produce significant movement in the hip frontal plane, in directions consistent with their moment arms. Finally, we conducted stochastic biomechanical model simulations to evaluate the influence that segment inertias, passive properties, and muscle moment arms have on muscle function in the sagittal and frontal planes.

II. Methods

A. Experimental Protocol

Ten healthy subjects (five males, five females; mean age 21 ± 2 years; height 1.71 ± 0.13 m; mass 72.85 ± 9.4 kg), with no history of musculoskeletal disorders were tested. All procedures were approved by the IRB of Northwestern University and complied with the principles of the Declaration of Helsinki. Informed consent was obtained prior to testing.

Subjects were positioned in swing phase postures using a computer-controlled robotic gait orthosis (Lokomat Hocoma Inc., Volketswil, Switzerland). Due to the prevalence of kinematic abnormalities during the swing phase of gait [1], four static postures were chosen ranging from toe-off (60% gait cycle) to just before heel strike (90% gait cycle). The subject's pelvis was securely strapped to the orthosis. Robotic actuators built-in to the gait orthosis were used to configure the hip and knee joints. The orthosis was fitted with two dof series elastic spring elements placed in series between the orthotic device and the right thigh and shank, so as to allow for sagittal and frontal plane movements (up to 5°) in response to electrical stimulation (compliant orthosis configuration, Fig. 1). Each spring was attached to a load cell (JR3 Inc., Woodland, CA) on the device in order to measure 3-D forces and moments exerted by the limb segments. For isometric torque measurements, a fixed orthosis configuration was used wherein the springs were removed and the load cells were rigidly attached between the limb segments and the orthosis.

Three muscles were selected for stimulation: RF, a muscle commonly targeted in treatment of hemiparetic gait [5], [12], [25]; BF, a representative biarticular hamstring muscle that has generated significant interest in other pathologies [24]; VL, a uniarticular quadriceps muscle with a knee extension moment arm that is slightly smaller than the RF. For each muscle, motor points were first determined using surface stimulation. Fine wire electrodes (50-μm-diameter nylon-coated nickel/chromium wire, California Wire Company, Grover Beach, CA) were then inserted into each muscle using two sterilized 25-gauge hypodermic needles approximately three inches apart. Ice and topical anesthetic cream were applied to highly sensitive areas prior to electrode insertion.

The electrical stimulation consisted of a stimulus train of four 0.3-ms pulses at 50 Hz (Compex Technologies Inc., New Brighton, MN). Three stimulus trains were administered at random times into each muscle at each of the four postures. The stimulus intensity was preset to the minimum amount necessary to produce peak forces that were at least six standard deviations above baseline force [26]. To facilitate comparison between quadriceps contributions, the stimulus intensity of the VL was chosen such that the peak torques at the knee were within 20% of the peak forces of the RF in the 70% gait cycle posture.

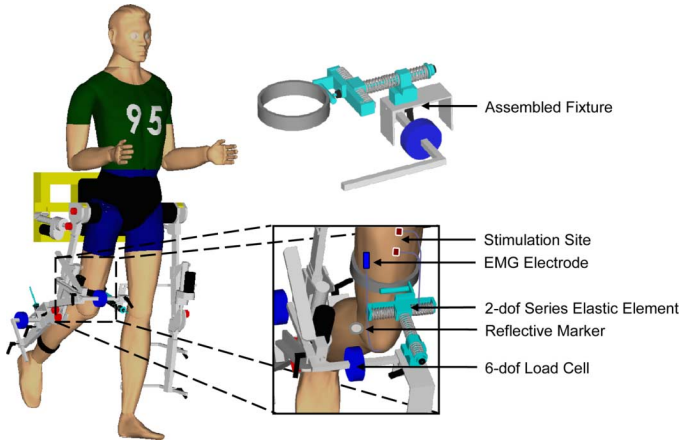

Fig. 1. Experimental setup for stimulation in compliant orthosis configuration. Assembled fixtures strapped to the thigh and shank each included a load cell to measure limb kinetics and series elastic element that permitted motion in sagittal and frontal planes. Intramuscular electrodes were inserted into the RF, BF, and VL. Surface electrodes were placed on stimulated and surrounding muscles to record electromyographic (EMG) activity. Three or more reflective markers were placed on each segment to track movement.

Prior to the electrical stimulation, subjects were instructed to maintain a relaxed state in all lower extremity muscles. Silver/silver chloride active surface electrodes (Motion Lab Systems, Baton Rouge, LA) recorded muscle activity in the BF, RF, VL, semitendinosus, and vastus medialis prior to and during the electrical stimulation. Trials with mean electromyographic (EMG) activity over two standard deviations above the baseline activity 100 ms before electrical stimulation were deemed unacceptable and rejected.

Prior to fitting in the orthotics, subjects were asked to stand quietly while an eight-camera motion capture system (Motion Analysis Corporation, Santa Rosa, CA) recorded the 3-D locations of sixteen retro reflective markers (12.7 mm diameter) affixed to the pelvis, right thigh, right shank, and right foot. Anatomical markers were placed on the posterior sacrum, the bilateral ASIS, greater trochanter, medial and lateral femoral condyles, medial and lateral malleoli, posterior heel counter of the shoe, and dorsally over the second metatarsal head to identify segment ends. An additional six reference markers rigidly affixed to thermoplastic shells (to minimize measurement error from skin movement), were wrapped securely to the posterior thigh and anterior shank. The mean of 300 frames of quiet standing data was used to calculate the relative position of the anatomical and reference markers. For the stimulation trials, marker trajectories were low-pass filtered at 6 Hz and used to track the 3-D motion of the pelvis and lower limb segments (EvaRT, Motion Analysis Corporation, Santa Rosa, CA). The relative positions and inter-segmental joint angles were calculated using a rigid body analysis [27].

Maximum voluntary contractions (MVCs) were performed while subjects were secured within the orthotic devise with series elastic elements removed (fixed orthosis configuration).

Authorized licensed use limited to: Queens University. Downloaded on February 23,2010 at 15:43:07 EST from IEEE Xplore. Restrictions apply.

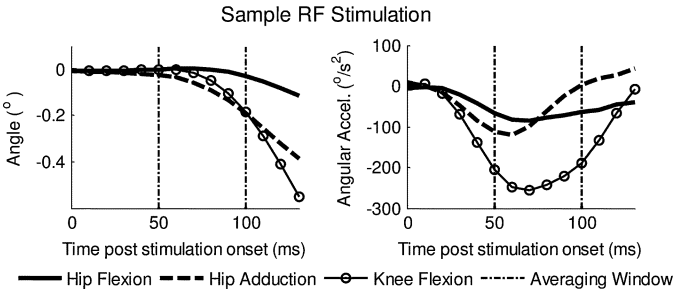

Fig. 2. Sample joint angle and angular acceleration time profiles of hip flexion, hip adduction, and knee flexion following onset RF stimulation. Vertical dashed lines indicate window used to determine average accelerations.

Load cell data were filtered offline using a fourth-order Butterworth, low-pass, and zero-phase digital filter with a 50-Hz cutoff frequency. To establish approximate induced muscle force, electrical stimulations of individual muscles were administered in multiple increments. Resulting torques at the knee, expressed as a percent of MVC, were used to estimate stimulation-induced muscle force.

In the compliant orthosis configuration, trials revealing limb movement (angle changes larger than six standard deviations from baseline) within a 20 ms window prior to stimulation were eliminated. Joint angles were numerically differentiated twice to obtain angular hip flexion/extension (HF/E), hip abduction/adduction (HAB/AD), and knee flexion/extension (KF/E) accelerations over time. Muscle-induced joint accelerations were defined as the average acceleration between 50 and 100 ms following the stimulus onset (Fig. 2). Directions of induced accelerations for each muscle were compared across subjects. To eliminate potential differences in the electrically-induced muscle force and to facilitate comparisons across subjects and muscles, acceleration ratios within the hip joint (HE/HAD) and between the hip and knee joints (HE/KE) were calculated.

B. Musculoskeletal Model

A generic lower extremity model [28] was used to estimate lower limb movement as a result of selective activation of muscles (SIMM Pipeline, Musculographics, Inc., Santa Rosa, CA; SD/FAST, Parametric Technology Corporation, Waltham, MA). The model included a pelvis (fixed), femur, and rigidly connected shank and foot allowing free motion at the hip (sagittal and frontal plane) and knee (sagittal plane). Dynamic simulations were performed for each muscle in each posture to replicate experimental trials. Following a muscle force perturbation, joint accelerations were calculated by numerically integrating equations of motion of the form

$$\ddot{\vec{q}} = I(q)^{-1}(R_{\rm ma}(q)\vec{F}_m + G(q)\mathrm{g} + V(q,\dot{q}) + T_{\rm ext}(q)) \quad (1)$$

where $q, \dot{q}, \ddot{q}$ are the joint angles, angular velocities and angular accelerations, I is the posture-dependent inertia matrix [29], [30], and $R_{\rm ma}$ is the muscle moment arm matrix. $\vec{F}_m$ is the force vector with a single nonzero term representing the approximate induced muscle force. G and V are the gravitational and coriolis/centripetal effects, respectively, and $T_{\rm ext}$ is the combined effect of passive and external spring torques. Initialization of the model included joint angles set to a given posture and joint velocities set to zero [22]. The passive torque contributions were initially neglected, whereas spring forces recorded during dynamic stimulation trials were used to calculate the external torque inputs, $T_{\rm ext}$. Model-predicted acceleration ratios (HE/HAD and HE/KE) were averaged over 50 ms and compared to average experimental ratios.

Normalization analyses in the fixed orthosis configuration were used to approximate the muscle forces induced by the electrical stimulation, $\vec{F}_m$, determined using the fixed orthosis configuration. For example, in the RF case, stimulation-induced torque at the knee ($\vec{T}_K$) was calculated using static equilibrium equations as follows:

$$\vec{T}_K = \sum_{i=1}^{2} \vec{d}_i \times \vec{F}_i + \vec{M}_i \quad (2)$$

where $\vec{M}_i$ and $\vec{F}_i$ are the measured moments and forces at the load cells and $\vec{d}_i$ is the posture-dependent distance vector from the knee joint to the ith load cell. Unlike the compliant configuration (Fig. 1), the othosis was instrumented with two load cells for the shank in the fixed orthosis configuration, hence the summation over two in (2). The joint torques following a knee MVC (in extension or flexion) were similarly measured and calculated using (2). The approximate percent of maximum force ($F^{\rm RF}_{\rm max}\%$) that was generated by the RF stimulation was calculated according to the following equation:

$$F^{\rm RF}_{\rm max}\% = \frac{F^{\rm RF}_{\rm stim}}{F^{\rm RF}_{\rm MVC}} \cdot 100 \approx \frac{T^{\rm RF}_{k\rm stim}}{T^{\rm all}_{k\rm MVC} \cdot C^{\rm RF}} \cdot 100 \quad (3)$$

where $T^{\rm RF}_{k\rm stim}$ is the measured knee torque following RF stimulation, which was divided by the product of $T^{\rm all}_{k\rm MVC}$ (the knee torque following a knee MVC with all muscles active), and $C^{\rm RF}$ (the torque contribution ratio of RF to all active muscles). This contribution ratio was the ratio of RF physiological cross sectional area (PCSA) to total PCSA of all active muscles, a measure of muscle volume shown to be representative of actual muscle force contribution [31]. Due to the isometric nature of this normalization procedure, it was assumed that percent knee torque was approximately equal to the ratio of muscle force generated by the stimulation ($F^{\rm RF}_{\rm stim}$) to maximum RF muscle force generated during an MVC ($F^{\rm RF}_{\rm MVC}$). This process was repeated for VL and BF muscles. Calculations in the static condition indicated that the stimulation induced muscle forces were approximately 5% of maximum muscle force (see [32] for details) and thus 5% was chosen as the input percent force for all dynamic simulations.

To examine the potential effect of subject-to-subject structural and anatomical differences unaccounted for in generic models, multiple simulations were performed using random modifications of segment masses, inertias, passive torques, and muscle moment arms. To assess the dynamic outcomes of reported segmental mass and inertial differences, thigh-to-shank mass ratio and thigh and shank inertial values were varied up to $\pm 20\%$ from the generic model values in increments of 1% [33], [34]. One thousand combinations of the three parameter values were randomly chosen from a uniform distribution to evaluate the effects of inertial differences on dynamic simulations.

Authorized licensed use limited to: Queens University. Downloaded on February 23,2010 at 15:43:07 EST from IEEE Xplore. Restrictions apply.

Combinations of passive joint torques were included in trial simulations for each muscle in each posture. Differential passive torques, $\delta T_j^{\mathrm{Pass}}$, were calculated using the following equations:

$$\delta T_{\mathrm{HF}}^{\mathrm{Pass}} = \alpha_{\mathrm{HF}} \cdot \delta\theta_{\mathrm{HF}} \tag{4}$$

$$\delta T_{\mathrm{KF}}^{\mathrm{Pass}} = \alpha_{\mathrm{KF}} \cdot \delta\theta_{\mathrm{KF}} \tag{5}$$

where $\delta\theta_j$ is the change in joint angle for a given dof, j, and α_j is the passive joint moment parameter varied up to $\pm 10\%$ of published sagittal plane passive torque values [35]. Since no known studies have documented frontal plane passive elastic hip joint torques, these contributions were modeled as a function of hip adduction, hip flexion, and knee flexion angles in the form

$$\delta T_{\mathrm{AD}}^{\mathrm{Pass}} = \alpha_{\mathrm{AD}} \cdot \delta\theta_{\mathrm{AD}} + \beta \cdot \left(\delta T_{\mathrm{HF}}^{\mathrm{Pass}} + \delta T_{\mathrm{KF}}^{\mathrm{Pass}}\right) \tag{6}$$

where α_{AD} is the passive joint parameter reflecting a direct influence of the HAB/AD degree-of-freedom and β is the parameter indicating the contribution of hip and knee sagittal plane angles on the frontal plane passive torque. The range of α_{AD} and value of β were chosen from within the range of sagittal plane parameters, α_{HF} and α_{KF}.

Considering subject-to-subject variability in anatomical features, hip and knee F/E moment arms are reported to vary as much as 26% and 33%, respectively [36]–[38]. However, few studies have explored the accuracy of modeled HAB/AD moment arms of the quadriceps and hamstrings. Alternatively, we estimated frontal plane moment arm ranges using a 10-mm-diameter sphere of feasible attachment locations surrounding the generic muscle, constrained by the maximum hip flexion and knee flexion moment arm variations reported in literature. One thousand random origin and insertion point iterations revealed HAB/AD moment arm changes of up to 85%. To determine the potential effects of these moment arm differences on dynamic outcomes, multiple simulations were performed using randomly selected muscle attachment sites. For each iteration, a total of six variables were changed simultaneously (three coordinates of muscle origin, three coordinates of muscle insertion) to generate HF/E, KF/E, and HAB/AD moment arm changes up to 26%, 33%, and 85%, respectively.

To examine the combined dynamic effects of the above factors, Monte Carlo simulations $(N = 1000)$ were performed with all twelve parameters (six attachment site coordinates, three inertial parameters, and three passive torque parameters) varying simultaneously [39], [40]. The span of all simulated acceleration ratios was used to assess the combined influence of theoretical lower limb subject-to-subject differences on the dynamic contributions of muscles.

A sensitivity analysis was used to estimate the affect of the aforementioned model parameters on the estimated acceleration ratios. Specifically, we computed the sensitivity as shown in (7), where the change in model output, ΔY, is defined as the magnitude change in estimated acceleration ratio (HE/HAD or HE/KE) as a result of the change in a given model parameter ΔP, and Y_o is the mean estimated acceleration ratio that corresponds to the nominal model parameter P_o. For example, let $R_o^{H/K}$ represent the estimated HE/KE acceleration ratio using the nominal model thigh-to-shank mass ratio $(M_o^{t/s})$ and $R^{H/K}$ represent the ratio using the perturbed mass ratio, $M^{t/s}$. The resulting sensitivity, S, was calculated as follows:

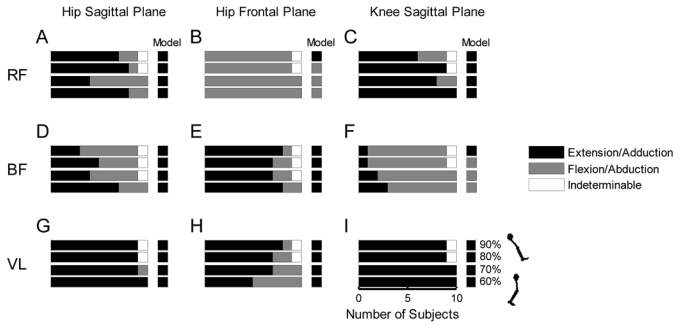

Fig. 3. Distribution of subject joint acceleration directions following muscle stimulation of RF (A)–(C), BF (D)–(F), and VL (G)–(I) for each degree-of-freedom (vertical columns) and each posture from 60% (toe-off) to 90% (heel strike) of gait cycle. Bars indicate number of subjects generating extension or adduction (black), flexion or abduction (grey) or indeterminable directions (white). Directions predicted by the *model* are indicated in squares to the right of each bar plot. Subjects exhibited consistent acceleration directions in RF and VL, and in general, were similar to model predictions.

$$S = \frac{\Delta Y / Y_o}{\Delta P / P_o} = \frac{\left(\dfrac{\sum_i^N \left|R^{H/K}(i) - R_o^{H/K}\right|}{\left|R_o^{H/K}\right|}\right)}{\left(\dfrac{\sum_i^N \left|M^{t/s}(i) - M_o^{t/s}\right|}{\left|M_o^{t/s}\right|}\right)} \tag{7}$$

where N is the number of iterations used. The formula given in (7) was also used to estimate the sensitivity of all model parameters discussed previously. Though sensitivity values were not normalized, they provided information on rank order of parameter sensitivities for a given muscle: a larger value indicated the output had a greater dependence on the specified parameter compared to others.

III. Results

A. Experimental Results

Stimulation of the RF, BF, and VL induced both sagittal and frontal plane motion about the hip. While accelerating the knee joint into extension, selective electrical stimulation of the RF also induced hip extension acceleration in an average of eight out of ten subjects at three of the four postures tested [Fig. 3(A) and (C)]. Data was less consistent across subjects for BF stimulation with averages (across all postures) of 48% and 78% of subjects producing hip extension and knee flexion acceleration, respectively [Fig. 3(D) and (F)]. The contributions of the stimulation-induced frontal plane hip accelerations were more consistent across subjects for both the RF and BF than the sagittal plane responses at the hip [Fig. 3(B) and (E) versus (A) and (D)]. Specifically, the RF and BF contributed to frontal plane motion with an average (across postures) of 95% of subjects exhibiting hip abduction acceleration following RF stimulation, and 75% exhibiting hip adduction acceleration following BF stimulation. As expected, the knee joint was accelerated into extension as a result of an electrical stimulation to the VL [Fig. 3(I)]. VL stimulation also resulted in hip extension acceleration in at least nine out of ten subjects and adduction acceleration in an average (across postures) of seven

Authorized licensed use limited to: Queens University. Downloaded on February 23,2010 at 15:43:07 EST from IEEE Xplore. Restrictions apply.

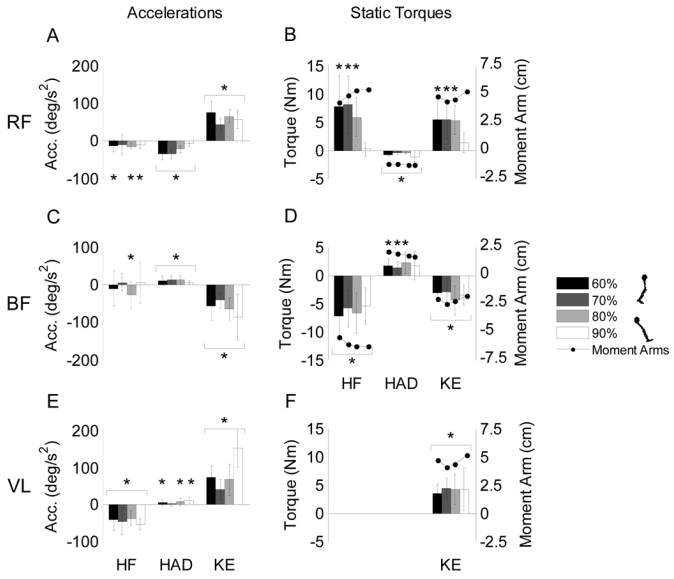

Fig. 4. Experimental mean and standard error accelerations (compliant orthosis configuration, left column) and static torques (fixed orthosis configuration, right column) for all three joint directions and all four postures (60%–90% left to right) following stimulation of RF (A),(B), BF (C),(D), and VL (E),(F). Positive values: HF, HAD, KE. Y-axis of moment arms (as calculated by generic musculoskeletal model) placed on right side of Static Torque plots. $(*)$ indicates not significantly different than zero $(\mathrm{alpha} = 0.05)$. RF and BF frontal plane directions remain consistent with moment arm directions for both static and dynamic cases. RF hip sagittal plane directions reverse and VL hip contributions become significant in dynamic settings.

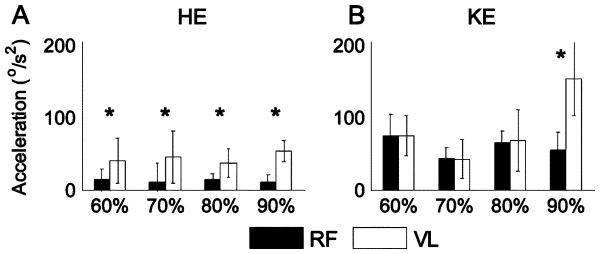

Fig. 5. Comparison of RF (black) and VL (white) experimental mean and standard error sagittal plane accelerations for (A) hip and (B) knee in all four postures. $(*)$ indicates significant difference, $\mathrm{alpha} = 0.05$). Both muscles exhibit similar knee accelerations; VL contributes roughly double the acceleration at the hip compared to that of RF.

out of ten subjects [Fig. 3(G) and (H)]. Both VL-induced hip and knee accelerations were posture independent.

Muscle torque and acceleration responses often differed between the fixed and compliant experimental conditions. During static stimulation trials, RF generated a hip flexion torque in the first three postures $(p < 0.005)$ consistent with its moment arm direction but induced hip extension acceleration in three postures (60%, 80%, and 90% of gait cycle) when the limb was in the compliant orthosis configuration $(p < 0.045)$. In the frontal plane, however, RF contributed to hip abduction in all postures of both the fixed $(p < 0.045)$ and compliant $(p < 0.005)$ configurations [Fig. 4(A) and (B)]. Mean hip adduction and extension torques observed during the fixed VL stimulation trials were statistically insignificant $(p > 0.072)$ in three out of four postures. However, in compliant configuration, the isolated electrical stimulation of the VL consistently accelerated the hip joint into extension [$p < 0.008$, Fig. 4(E)]. In the fixed orthosis configuration, BF generated torques about the hip and knee that were consistent with its anatomical classification for all postures of hip extension $(p < 0.008)$, for first three postures of hip adduction $(p < 0.029)$, and for all postures of knee flexion $(p < 0.010)$ [Fig. 4(D)]. However, in the compliant configuration, there was large variability in hip sagittal plane accelerations (normalized standard deviation of 0.36 for accelerations as opposed to 0.07 for torques) [Fig. 4(C)].

Under the fixed orthosis configuration, our data revealed no difference in knee extension torques following electrical stimulation of the RF and VL for the first three postures as shown in Fig. 4(B) and (F) $(p > 0.162)$. Consistent with the static torque similarities, the difference between the RF and VL induced knee accelerations were statistically insignificant in the same three postures as shown in Fig. 5(B) $(p > 0.848)$. These comparable results indicated that the contribution of the shank extension mechanics to the *knee* induced accelerations is equivalent for both muscles. However, comparison at the *hip* revealed VL-induced hip accelerations were significantly larger than RF-induced hip accelerations $(p < 0.049)$ [Fig. 5(A)].

B. Comparison to Model Predictions

The generic musculoskeletal model predicted RF, BF, and VL to accelerate the hip into extension when selectively activated in all configurations tested [Fig. 3(A), (D), and (G)]. Hip frontal plane acceleration predictions were consistent with anatomical classifications for both biarticular muscles RF (with the exception of the 90% posture) and BF [Fig. 3(B) and (E)]. Additionally, the VL was predicted to adduct the hip in all postures [Fig. 3(H)]. Finally, knee sagittal plane acceleration predictions were consistent with anatomical classifications for all muscles (with the exception of BF in the 90% posture) [Fig. 3(C), (F), and (I)].

Though capable of predicting the sign of the electrically induced accelerations for the majority of postures, the generic musculoskeletal model was less consistent in predicting the experimentally observed acceleration ratios (Fig. 6). Using the nominal set of parameters in SIMM and neglecting passive torques, the RF and VL model-predicted ratios in the sagittal plane (HE/KE) were generally within one standard error of the experimentally observed ratios across postures [Fig. 6(A) and (E)]. However the BF predicted sagittal acceleration ratios were generally smaller (average of four standard errors) than their experimentally observed counterparts [Fig. 6(C)]. The HE/HAD model-predicted ratios were generally much greater (up to 280 standard errors greater for RF, 23 standard errors for VL) than the experimental ratios for the quadriceps [Fig. 6(B) and (F)]. Conversely, the predicted HE/HAD ratios were significantly smaller $(p < 0.023)$ than the experimentally observed ratios for the BF muscle [Fig. 6(D)]. In this case, both the model-predicted and experimental ratios showed similar dependence on posture (correlation coefficient 0.99). It is important to note that the model-based ratios were

Authorized licensed use limited to: Queens University. Downloaded on February 23,2010 at 15:43:07 EST from IEEE Xplore. Restrictions apply.

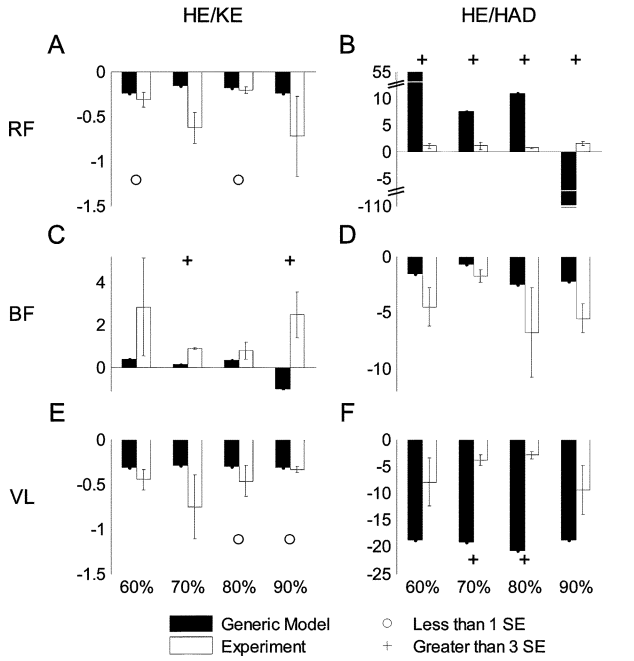

Fig. 6. Generic model (black) and experimental (white) acceleration ratios with standard error bars for all four postures of HE/KE sagittal plane ratios (left column) and HE/HAD hip joint ratios (right column); RF (A), (B), BF (C), (D), and VL (E), (F) in each posture. In general, RF and VL HE/KE acceleration ratios predictions are similar to those experimentally observed whereas HE/HAD predicted ratios were much larger than observed.

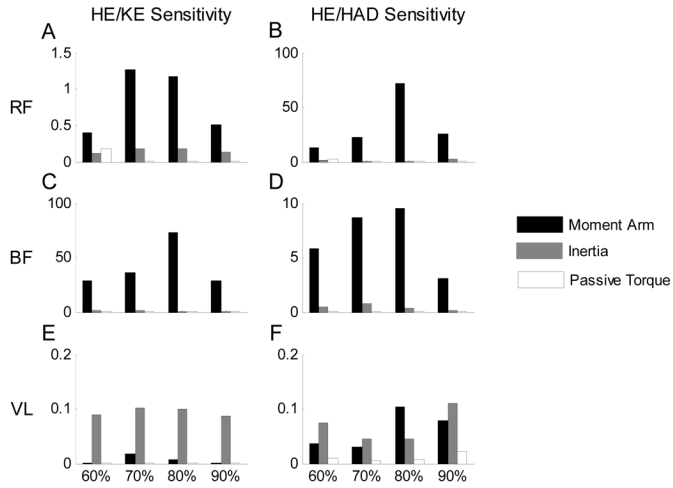

Fig. 7. Single-factor sensitivities of RF (A), (B), BF (C), (D) and VL (E), (F) for HE/KE sagittal plane ratios (left column) and HE/HAD hip joint ratios (right column). Sensitivities are provided for each parameter variation: moment arms (black), inertial properties of the thigh and shank (grey), and passive joint torques (white). For RF and BF, moment arm variations have significantly higher sensitivities than inertial properties and passive joint torques.

in the opposite direction at the 90% posture for BF HE/KE and for the RF HE/HAD ratios.

C. Sensitivity Analysis

Multifactor Monte Carlo based simulations resulted in acceleration ratios that improved to within one standard error of observed value in two postures for RF HE/HAD ratios, all four postures for BF HE/HAD ratios, and three postures for BF HE/KE ratios. In two postures of the RF and VL muscles, model HE/KE acceleration ratios were within one standard error using the nominal set of parameters and remained within one standard error for all iterations. In all other postures, no iterations demonstrated ratio improvement to within one standard error.

Single-factor sensitivity analyses using (7) demonstrated that the mean sensitivity (across postures and parameters) of MA variation in the RF HE/KE acceleration ratio was 0.84, whereas mean sensitivities of inertia and passive torque properties were below 0.15 [Fig. 7(A)]. For HE/HAD ratios, mean sensitivity of MA variation in RF was 33.5, whereas mean sensitivities of other parameters were less than 1.40 [Fig. 7(B)]. Similarly, greater sensitivity values for moment arm parameters were observed in the BF ratios. Mean sensitivity of MA variation in BF HE/KE and HE/HAD ratios were 41.9 and 6.80, respectively, with inertia and passive torque mean sensitivities less than 1.23 [Fig. 7(C) and (D)]. For VL, average sensitivities of inertial property variations were largest for HE/KE ratios (0.09) as opposed to MA and passive torque variations [6.80e-3, 4.00e-4, respectively, Fig. 7(E)]. In the HE/HAD ratio, both MA and inertial property sensitivities were similar in average value (0.068, 0.062, respectively) and larger than the mean sensitivity for passive torque variation (0.01) [Fig. 7(F)].

IV. Discussion

In this study, we sought to examine the dynamic contributions of quadriceps and hamstring muscles through selective electrical stimulation in swing phase postures. Muscles often demonstrated counterintuitive mechanical function at the hip, demonstrating the need to consider intersegmental interactions in addition to a muscle's anatomical structure when assessing function. Specifically, activation of the RF accelerated the hip joint into extension, a function that is opposite to the muscle's experimentally observed static flexion torque at the hip. Hip extension was also observed when the uniarticular VL was selectively activated, which is attributable to intersegmental forces at the knee elicited by VL force. These findings are consistent with a recent experimental investigation acquired in supine subjects [22] as well as computational studies [14], [21]. Our data also revealed that lower limb sagittal plane muscles made contributions to the frontal plane dynamics that were significant when compared to their sagittal plane function. Hip frontal plane acceleration directions of the biarticular muscles (RF and BF) were consistent with their experimentally observed static torques as well as their predicted frontal plane moment arms [41].

Under conditions producing similar mechanical interactions at the knee, VL produced about twice the hip extension acceleration compared to RF. Though this finding is not acknowledged in literature, there is a logical rationale. VL and RF generate similar knee extension moments (per unit force) which will have the same effect at the hip (e.g., hip extension in early swing). However, RF also generates a hip flexion moment which would contribute to hip flexion acceleration. Thus the contribution of VL to net hip extension acceleration should exceed that of RF. This finding emphasizes the significance of the dynamic coupling interaction on determining the dynamic function of a biarticular muscle.

Authorized licensed use limited to: Queens University. Downloaded on February 23,2010 at 15:43:07 EST from IEEE Xplore. Restrictions apply.

Further examination through dynamic simulations revealed that although the musculoskeletal model can generally indicate the correct signs of 3-D muscle contributions, the accuracy of relative acceleration predictions is limited by model generalities. Single- and multi-factor analyses revealed that for select muscles, simulation-based outcomes are highly sensitive to muscle moment arms: following certain variations to RF or BF moment arm values, the model was capable of producing accelerations within experimentally observed ranges. Thus, although subject differences in inertial properties and passive torques may play a minor role, acceleration predictions are primarily influenced by musculoskeletal model moment arm accuracy.

A. Isometric Hip Torques

Hip flexion torque induced by RF stimulation was substantially larger at toe-off limb postures than late swing limb postures (i.e., insignificant HF at 90%, $p = 0.184$). This decrease was accompanied with a persistent reduction in the RF knee extension torque as the lower limb configuration progressed to the heel strike posture (i.e., insignificant KE at 90%, $p = 0.0537$) [Fig. 4(B)]. These torque producing capabilities cannot be a result of changes in muscle moment arms, since the RF hip flexion and knee extension moment arms increase as posture progresses from toe-off to heel strike [37]. Alternatively, the decrease in torque can be attributed to the 35% decrease in RF active force capacity in late swing postures due to its shortened and slack state (SIMM, [42]). Furthermore, it is possible that the observed reduction of the RF hip and knee static torques may have been attributed to differences in the number of fibers recruited across postures [43]–[45]. In any case, in the context of the current study, the acceleration ratio is unaffected by such differences in moment production capabilities of the muscles of interest.

B. Hip Acceleration Variability

Significant differences were observed between the predicted across-plane hip ratios of VL and experimentally observed values that could not be accounted for with MA or inertial parameter variation. One could argue that observed accelerations may have been confounded by electrical spillover, i.e., induced activations of neighboring muscles. However, the use of fine-wire electrodes as well as a cross-correlation analysis of surface EMG confirmed the absence of untargeted muscle activation. Alternatively, it has been suggested that following muscle contraction, rotation of the femur with respect to the patella may bring about a directional change in the intersegmental mechanical interactions [46]. Without fixed femoral rotation, it is plausible that activation of the VL muscle may have resulted in a femoral rotation that when coupled with the irregular geometry of the femur, may have manifested in appreciable abduction/adduction acceleration at the hip. Such interactions were not captured by the model simulations. It is also important to note that in the single-factor sensitivity analysis, the RF and BF had moment arms at both the hip and knee which yielded higher sensitivities to acceleration results, than moment arm variations of the knee alone in the VL [Fig. 7(E) and (F)]. Further investigation is necessary to determine the underlying factors contributing to the inaccurate model-based hip acceleration ratio predictions following contraction of the uniarticular VL.

Large subject-to-subject variability was observed in hip extension accelerations following unconstrained hamstrings stimulation ($p > 0.26$, 60%, 70%, 90% postures). The majority of subjects indicated greater sensitivity to stimulation of the BF compared to the quadriceps muscles, perhaps due to proximity of cutaneous nerves. One could argue that if the electrodes were near pain receptors, the stimulus may have induced a reflex withdrawal response causing flexion of the hip. However, significant movement response to this stimulation typically occurs 125–300 ms following the stimulus, well after the timeframe observed for accelerations [45]. It is possible that monosynaptic stretch reflexes arose in neighboring muscles contributing to the observed acceleration of the limb. However, a cross-correlation analysis of muscle EMG revealed strong association between the first pulse and each consecutive pulse window where reflex activity would be expected, making it highly unlikely that reflexive-based forces were present in the applicable timeframe. A more plausible explanation for the variability in BF hip action is sensitivity in the muscle's moment arm. In the neutral hip position, the BF moment arm is over 30% greater than the RF moment arm, thus changes to its value via muscle attachment sites would have a larger effect on the net action at the hip than changes to the RF moment arm. This was supported by sensitivity analyses which revealed large variances in output accelerations following small changes in moment arm compared to inertial and passive force changes [Fig. 7(C), (D)]. Though the use of ten subjects provided statistically significant results across the RF and VL, a future investigation with larger sample size may be necessary to provide sufficient data to confidently predict BF dynamic function during swing.

C. Biomechanical Implications

One could argue that the dynamic function of muscles during *continuous* movement could be substantially different than data obtained in this study. Induced acceleration analysis provides an instantaneous estimate of a muscle's capacity to induce movement, and is only dependent on the current body configuration. Our experimental methods employ the calculation of induced acceleration by considering how motion is induced across time, so there is the potential for movement to affect the results. Though it is difficult to speculate how the outcomes would change in the dynamic state, results of a recent study have shown that experimental measures of soleus and gastrocnemius function during gait were consistent with the direction of induced acceleration predictions, suggesting that positional effects may indeed have the greatest influence on the induced movement in stimulation experiments of the type conducted [23].

In addition to counterintuitive sagittal plane function of muscles, one key outcome of this investigation is the significant frontal plane contribution of the RF, BF, and VL. Specifically, the observed frontal to sagittal plane acceleration ratios for RF, BF, and VL were approximately 1:1, 1:5, and 1:6, respectively. These findings are important when considering the generalized 3-D function of muscles in the context of current rehabilitation interventions in patients with neurological disorders. Such interventions include muscle-tendon transfer surgeries (e.g., [47]–[49]), pharmacological injections (e.g., [2], [3], [50]), and FES (e.g., [51]–[53]). For example, the RF is often targeted to reduce stiff-knee gait post stroke [3]. Indeed, the selective weakening of the RF has been shown to promote knee flexion;

Authorized licensed use limited to: Queens University. Downloaded on February 23,2010 at 15:43:07 EST from IEEE Xplore. Restrictions apply.

however, potential effects of this acute weakening of the RF on the hip joint's 3-D movements have not been examined. Similarly, FES-assisted therapy has been shown to improve stroke gait abnormalities by targeting hamstrings and quadriceps muscles [54]. However, kinematic analysis is thus far limited to the sagittal plane; potential influence of such activations on the frontal plane movements is less understood.

Musculoskeletal models are increasingly used to investigate underlying biomechanical factors in gait abnormalities following neurological disorders. A significant number of these disorders are characterized by excessive frontal plane movements. However, most of the existing model-based analyses of such pathologies have been limited to the sagittal plane mechanics [55]–[57]. Given the significant 3-D interactions presented in this study, we argue that special attention should be given to the use of generic musculoskeletal models in the study of pathological gait. Specifically, our data has shown significant differences between experimental and predicted dynamic muscle function in the frontal plane. Sensitivity analyses have revealed that this effect is highly dependent on the choice of the abduction/adduction moment arms of the muscles spanning the hip joint under isolated simulation conditions. Taken together, our findings illustrate the importance of considering intersegmental dynamics and muscle moment arms when using musculoskeletal modeling for the study of 3-D pathological gait.

ACKNOWLEDGMENT

The authors would like to thank W. Lin and M. Donoghue for their assistance with data collection and analysis.

REFERENCES

[1] D. C. Kerrigan, E. P. Frates, S. Rogan, and P. O. Riley, "Hip hiking and circumduction: Quantitative definitions," *Am. J. Phys. Med. Rehabil.*, vol. 79, pp. 247–252, 2000.

[2] D. J. Wilson, M. K. Childers, D. L. Cooke, and B. K. Smith, "Kinematic changes following botulinum toxin injection after traumatic brain injury," *Brain Injury*, vol. 11, pp. 157–167, 1997.

[3] D. H. Sung and H. J. Bang, "Motor branch block of the rectus femoris: Its effectiveness in stiff-legged gait in spastic paresis," *Arch. Phys. Med. Rehabil.*, vol. 81, pp. 910–915, 2000.

[4] M. Rousseaux, S. Compere, M. J. Launay, and O. Kozlowski, "Variability and predictability of functional efficacy of botulinum toxin injection in leg spastic muscles," *J. Neurol. Sci.*, vol. 232, pp. 51–57, 2005.

[5] F. Chantraine, C. Detrembleur, and T. M. Lejeune, "Effect of the rectus femoris motor branch block on post-stroke stiff-legged gait," *Acta Neurologica Belgica*, vol. 105, pp. 171–177, 2005.

[6] C. A. Johnson, J. H. Burridge, P. W. Strike, D. E. Wood, and I. D. Swain, "The effect of combined use of botulinum toxin type A and functional electric stimulation in the treatment of spastic drop foot after stroke: A preliminary investigation," *Arch. Phys. Med. Rehabil.*, vol. 85, pp. 902–909, 2004.

[7] J. J. Daly and R. L. Ruff, "Electrically induced recovery of gait components for older patients with chronic stroke," *Am. J. Phys. Med. Rehabil.*, vol. 79, pp. 349–360, 2000.

[8] J. J. Daly, K. Roenigk, P. J. Holcomb, J. M. Rogers, K. Butler, J. Gansen, J. McCabe, E. Fredrickson, E. B. Marsolais, and R. L. Ruff, "A randomized controlled trial of functional neuromuscular stimulation in chronic stroke subjects," *Stroke*, vol. 37, pp. 172–178, 2006.

[9] G. Yavuzer, D. Geler-Kulcu, B. Sonel-Tur, S. Kutlay, S. Ergin, and H. J. Stam, "Neuromuscular electric stimulation effect on lower-extremity motor recovery and gait kinematics of patients with stroke: A randomized controlled trial," *Arch. Phys. Med. Rehabil.*, vol. 87, pp. 536–540, 2006.

[10] S. Hesse, M. T. Jahnke, D. Luecke, and K. H. Mauritz, "Short-term electrical stimulation enhances the effectiveness of Botulinum toxin in the treatment of lower limb spasticity in hemiparetic patients," *Neurosci. Lett.*, vol. 201, pp. 37–40, 1995.

[11] S. Ozcakir and K. Sivrioglu, "Botulinum toxin in poststroke spasticity," *Clin. Med. Res.*, vol. 5, pp. 132–138, 2007.

[12] G. D. Caty, C. Detrembleur, C. Bleyenheuft, T. Deltombe, and T. M. Lejeune, "Effect of simultaneous botulinum toxin injections into several muscles on impairment, activity, participation, and quality of life among stroke patients presenting with a stiff knee gait," *Stroke*, vol. 39, pp. 2803–2808, 2008.

[13] G. G. Stoquart, C. Detrembleur, S. Palumbo, T. Deltombe, and T. M. Lejeune, "Effect of botulinum toxin injection in the rectus femoris on stiff-knee gait in people with stroke: A prospective observational study," *Arch. Phys. Med. Rehabil.*, vol. 89, pp. 56–61, 2008.

[14] S. J. Piazza and S. L. Delp, "The influence of muscles on knee flexion during the swing phase of gait," *J. Biomech.*, vol. 29, pp. 723–733, 1996.

[15] F. E. Zajac, R. R. Neptune, and S. A. Kautz, "Biomechanics and muscle coordination of human walking. Part I: Introduction to concepts, power transfer, dynamics and simulations," *Gait Posture*, vol. 16, pp. 215–232, 2002.

[16] F. E. Zajac, R. R. Neptune, and S. A. Kautz, "Biomechanics and muscle coordination of human walking: Part II: Lessons from dynamical simulations and clinical implications," *Gait Posture*, vol. 17, pp. 1–17, 2003.

[17] F. C. Anderson and M. G. Pandy, "Dynamic optimization of human walking," *J. Biomech. Eng.*, vol. 123, pp. 381–390, 2001.

[18] I. Jonkers, C. Stewart, and A. Spaepen, "The study of muscle action during single support and swing phase of gait: Clinical relevance of forward simulation techniques," *Gait Posture*, vol. 17, pp. 97–105, 2003.

[19] F. E. Zajac and M. E. Gordon, "Determining muscle's force and action in multi-articular movement," *Exercise Sport Sci. Rev.*, vol. 17, pp. 187–230, 1989.

[20] A. S. Arnold, F. C. Anderson, M. G. Pandy, and S. L. Delp, "Muscular contributions to hip and knee extension during the single limb stance phase of normal gait: A framework for investigating the causes of crouch gait," *J. Biomech.*, vol. 38, pp. 2181–2189, 2005.

[21] R. R. Neptune, F. E. Zajac, and S. A. Kautz, "Muscle force redistributes segmental power for body progression during walking," *Gait Posture*, vol. 19, pp. 194–205, 2004.

[22] A. Hernandez, Y. Dhaher, and D. G. Thelen, "In vivo measurement of dynamic rectus femoris function at postures representative of early swing phase," *J. Biomech.*, 2007.

[23] C. Stewart, N. Postans, M. H. Schwartz, A. Rozumalski, and A. Roberts, "An exploration of the function of the triceps surae during normal gait using functional electrical stimulation," *Gait Posture*, vol. 26, pp. 482–488, 2007.

[24] C. Stewart, N. Postans, M. H. Schwartz, A. Rozumalski, and A. P. Roberts, "An investigation of the action of the hamstring muscles during standing in crouch using functional electrical stimulation (FES)," *Gait Posture*, vol. 28, pp. 372–377, 2008.

[25] J. V. Robertson, D. Pradon, D. Bensmail, C. Fermanian, B. Bussel, and N. Roche, "Relevance of botulinum toxin injection and nerve block of rectus femoris to kinematic and functional parameters of stiff knee gait in hemiplegic adults," *Gait Posture*, 2008.

[26] B. V. Hunter, D. G. Thelen, and Y. Dhaher, "Experimental evaluation of model-based lower extremity induced accelerations," in *Amer. Soc. Biomechan. Conf.*, 2007.

[27] E. S. Grood and W. J. Suntay, "A joint coordinate system for the clinical description of three-dimensional motions: Application to the knee," *J. Biomech. Eng.*, vol. 105, pp. 136–144, 1983.

[28] S. Delp, J. Loan, M. Hoy, F. Zajac, E. Topp, and J. Rosen, "An interactive graphics-based model of the lower extremity to study orthopaedic surgical procedures," *IEEE Trans. Biomed. Eng.*, vol. 37, no. 8, pp. 757–767, Aug. 1990.

[29] P. de Leva, "Adjustments to Zatsiorsky-Seluyanov's segment inertia parameters," *J. Biomech.*, vol. 29, pp. 1223–1230, 1996.

[30] D. Lafond, H. Corriveau, and F. Prince, "Postural control mechanisms during quiet standing in patients with diabetic sensory neuropathy," *Diabetes Care*, vol. 27, pp. 173–178, 2004.

[31] S. E. Alway, J. Stray-Gundersen, W. H. Grumbt, and W. J. Gonyea, "Muscle cross-sectional area and torque in resistance-trained subjects," *Eur. J. Appl. Physiol. Occup. Physiol.*, vol. 60, pp. 86–90, 1990.

[32] R. A. Brand, D. R. Pedersen, and J. A. Friederich, "The sensitivity of muscle force predictions to changes in physiologic cross-sectional area," *J. Biomech.*, vol. 19, pp. 589–596, 1986.

Authorized licensed use limited to: Queens University. Downloaded on February 23,2010 at 15:43:07 EST from IEEE Xplore. Restrictions apply.

[33] J. L. Durkin and J. J. Dowling, "Body segment parameter estimation of the human lower leg using an elliptical model with validation from DEXA," *Ann. Biomed. Eng.*, vol. 34, pp. 1483–1493, 2006.
[34] V. Zatsiorsky, V. Seluyanov, and L. Chugunova, "Methods of determining mass-inertial characteristics of human body segments," *Contemp.Problems Biomechan.*, pp. 272–291, 1990.
[35] R. Riener and T. Edrich, "Identification of passive elastic joint moments in the lower extremities," *J. Biomech.*, vol. 32, pp. 539–544, 1999.
[36] A. S. Arnold, S. Salinas, D. J. Asakawa, and S. L. Delp, "Accuracy of muscle moment arms estimated from MRI-based musculoskeletal models of the lower extremity," *Computer Aided. Surg.*, vol. 5, pp. 108–119, 2000.
[37] W. L. Buford Jr., F. M. Ivey Jr., J. D. Malone, R. M. Patterson, G. L. Peare, D. K. Nguyen, and A. A. Stewart, "Muscle balance at the knee—Moment arms for the normal knee and the ACL-minus knee," *IEEE Trans. Rehabil. Eng.*, vol. 5, no. 4, pp. 367–379, Apr. 1997.
[38] M. Ito, H. Akima, and T. Fukunaga, "In vivo moment arm determination using B-mode ultrasonography," *J. Biomech.*, vol. 33, pp. 215–218, 2000.
[39] Y. Y. Dhaher, "Joint-afferent-mediated muscle activations yield a near-maximum torque response of the quadriceps," *J. Neurosci. Methods*, vol. 133, pp. 1–17, 2004.
[40] S. G. McLean, A. Su, and A. J. van den Bogert, "Development and validation of a 3-D model to predict knee joint loading during dynamic movement," *J. Biomech. Eng.*, vol. 125, pp. 864–874, 2003.
[41] L. L. Menegaldo, A. de Toledo Fleury, and H. I. Weber, "Moment arms and musculotendon lengths estimation for a three-dimensional lower-limb model," *J. Biomech.*, vol. 37, pp. 1447–1453, 2004.
[42] F. C. Anderson and M. G. Pandy, "A dynamic optimization solution for vertical jumping in three dimensions," *Comput. Methods Biomech. Biomed. Eng.*, vol. 2, pp. 201–231, 1999.
[43] R. M. Enoka and A. J. Fuglevand, "Motor unit physiology: Some unresolved issues," *Muscle Nerve*, vol. 24, pp. 4–17, 2001.
[44] C. M. Gregory and C. S. Bickel, "Recruitment patterns in human skeletal muscle during electrical stimulation," *Phys. Therapy*, vol. 85, pp. 358–364, 2005.
[45] G. Sandrini, M. Serrao, P. Rossi, A. Romaniello, G. Cruccu, and J. C. Willer, "The lower limb flexion reflex in humans," *Prog. Neurobiol.*, vol. 77, pp. 353–395, 2005.
[46] C. M. Powers, Y. J. Chen, I. Scher, and T. Q. Lee, "The influence of patellofemoral joint contact geometry on the modeling of three dimensional patellofemoral joint forces," *J. Biomech.*, vol. 39, pp. 2783–2791, 2006.
[47] D. S. Asakawa, S. S. Blemker, G. E. Gold, and S. L. Delp, "In vivo motion of the rectus femoris muscle after tendon transfer surgery," *J. Biomechan.*, vol. 35, pp. 1029–, 2002.
[48] S. Morita, H. Yamamoto, and K. Furuya, "Anterior transfer of the toe flexors for equinovarus deformity due to hemiplegia," *J. Bone. Joint. Surg. Br.*, vol. 76-B, pp. 447–449, 1994.
[49] S. J. Piazza, R. L. Adamson, J. O. Sanders, and N. A. Sharkey, "Changes in muscle moment arms following split tendon transfer of tibialis anterior and tibialis posterior," *Gait Posture*, vol. 14, pp. 271–278, 2001.
[50] F. Chantraine, C. Detrembleur, and T. M. Lejeune, "Effect of the rectus femoris motor branch block on post-stroke stiff-legged gait.," *Acta Neurologica Belgica*, vol. 105, pp. 171–177, 2005.
[51] J. J. Daly, K. L. Roenigk, K. M. Butler, J. L. Gansen, E. Fredrickson, E. B. Marsolais, J. Rogers, and R. L. Ruff, "Response of sagittal plane gait kinematics to weight-supported treadmill training and functional neuromuscular stimulation following stroke," *J. Rehabil. Res. Develop.*, vol. 41, pp. 807–820, 2004.
[52] M. Glanz, S. Klawansky, W. Stason, C. Berkey, and T. C. Chalmers, "Functional electrostimulation in poststroke rehabilitation: A meta-analysis of the randomized controlled trials," *Arch. Phys. Med. Rehabil.*, vol. 77, pp. 549–553, 1996.
[53] T. A. Thrasher and M. R. Popovic, "Functional electrical stimulation of walking: Function, exercise and rehabilitation," *Ann. Readapt. Med. Phys.*, vol. 51, pp. 452–460, 2008.
[54] J. J. Daly, K. Sng, K. Roenigk, E. Fredrickson, and M. Dohring, "Intra-limb coordination deficit in stroke survivors and response to treatment," *Gait Posture*, vol. 25, pp. 412–418, 2007.
[55] K. Parvataneni, S. J. Olney, and B. Brouwer, "Changes in muscle group work associated with changes in gait speed of persons with stroke," *Clin. Biomech. (Bristol, Avon)*, vol. 22, pp. 813–820, 2007.
[56] P. O. Riley and D. C. Kerrigan, "Torque action of two-joint muscles in the swing period of stiff-legged gait: A forward dynamic model analysis," *J. Biomechan.*, vol. 31, pp. 835–, 1998.
[57] G. O. Young, "Synthetic structure of industrial plastics," in *Plastics*, J. Peters, Ed., 2nd ed. New York: McGraw-Hill, 1964, vol. 3, pp. 15–64.

Betsy V. Hunter received the B.S. degree in engineering, biomedical concentration *(summa cum laude)* from LeTourneau University, Longview, TX, in 2004, and the M.S. degree in biomedical engineering, in 2008, from Northwestern University, Evanston, IL, where she is currently working toward the Ph.D. degree in biomedical engineering.

She has participated in the research of lower limb gait abnormalities as a member of the Neuromechanics of Impaired Locomotion Laboratory in the Sensory Motor Performance Program at the Rehabilitation Institute of Chicago, Chicago, IL, since 2004. Her research interests include the development of computational models to simulate lower limb gait mechanics for exploration of potential rehabilitation strategies.

Ms. Hunter has received a Graduate Research Fellowship from the National Institutes of Health as well as a Predoctoral Fellowship from the American Heart Association. She is a member of the American Society of Biomechanics.

Darryl G. Thelen received the B.S. degree in mechanical engineering from Michigan State University, East Lansing, MI, in 1987 and the M.S.E. and Ph.D. degrees in mechanical engineering from the University of Michigan, Ann Arbor, MI, in 1988 and 1992, respectively.

He worked as a Post-Doctoral Fellow at the University of Michigan from 1992 to 1994, as an Assistant Professor of engineering at Hope College, Holland, MI, from 1994 to 2000, as a visiting faculty member at Stanford University, Stanford, CA, from 2000 to 2001, and as a Principal Engineer at Honda Fundamental Research Laboratories, Mountain View, CA, from 2001 to 2002. Since 2002, he has been on the faculty of the Department of Mechanical Engineering at the University of Wisconsin-Madison, where he is currently an Associate Professor. His research interests include computational biomechanics, simulation and control of human locomotion, and dynamic imaging of musculotendon mechanics. Clinical applications include rehabilitation following muscle injury and the treatment of gait impairments associated with aging and disease.

Dr. Thelen was awarded a Faculty Early Career Development (CAREER) Award by the National Science Foundation. He has been a member of the American Society of Mechanical Engineers since 1992 and of the American Society of Biomechanics since 1995.

Yasin Y. Dhaher (SM'08) received the B.S. and M.Sc. degrees in mechanical engineering from Yarmouk and Jordan University of Science and Technology, Irbid, Jordan, in 1987 and 1990, respectively, and the Ph.D. degree in theoretical mechanics from Michigan State University, East Lansing, , in 1997.

He holds faculty appointments in the Physical Medicine and Rehabilitation Department and the Biomedical Engineering Department of Northwestern University, Evanston, IL, and a Senior Research Scientist position at the Sensory Motor Performance Program (SMPP) at The Rehabilitations Institute of Chicago, Chicago, IL. He is the Director of the Joint Neuromechanics, and the Neuromechanics of Impaired Locomotion Laboratories at SMPP. He chairs the Biomechanics Core Curriculum Committee at the Biomedical Engineering Department, Northwestern University. His research is focused on two related topics: biomechanics and motor control. Using computational and experimental approaches, the primary goal of his investigations is to evaluate and improve rehabilitations interventions after neurological and musculoskeletal disabilities.

Dr. Dhaher serves on the Editorial Board of the IEEE TRANSACTIONS ON BIOMEDICAL ENGINEERING and the *International Journal of Experimental and Computational Biomechanics*.

Authorized licensed use limited to: Queens University. Downloaded on February 23,2010 at 15:43:07 EST from IEEE Xplore. Restrictions apply.